



Olefin epoxidation with ionic liquid catalysts formed by supramolecular interactions

Bingjie Ding^a, Ran Zhang^b, Qingqing Zhou^a, Wenbao Ma^a, Anna Zheng^a, Difan Li^a, Yefeng Yao^{b,*}, Zhenshan Hou^{a,*}

^a Key Laboratory for Advanced Materials, Research Institute of Industrial Catalysis, East China University of Science and Technology, Shanghai 200237, China

^b Physics Department and Shanghai Key Laboratory of Magnetic Resonance, East China Normal University, Shanghai 200062, China

ARTICLE INFO

Keywords:

Ionic liquid
Peroxoniobate
Crown ether
Supramolecular interaction
Olefin epoxidation

ABSTRACT

This work demonstrated that the specific ionic liquids (ILs) have been designed via the supramolecular complexation between 18-crown-6 (CE) and ammonium peroxyoxoniobate (NH₄-Nb). The resultant ILs have been characterized by elemental analysis, FT-IR, Raman, NMR, DSC, conductivity measurement and MALDI-TOF, etc. The IL (CE-1) consisting of CE and ammonium peroxyoxoniobate can be further coordinated with GLY to generate a new IL (CE-2), which showed both high catalytic activity in epoxidation with H₂O₂ and good recyclability. The characterization of ⁹³Nb NMR spectra revealed that the peroxyoxoniobate anions has demonstrated a structural evolution in the presence of hydrogen peroxide, in which Nb=O species can be easily oxidized into the catalytically active niobium-peroxy species. Especially, the supramolecular complexation can provide suitable hydrophobicity, which ensured that the hydrophobic olefins and allylic alcohols were easily accessible to the catalytically active anions, and thus facilitated the epoxidation reaction. Notably, the supramolecular IL catalysts in this work exhibited a huge advantage of the easy availability, as compared with the previously reported peroxyoxoniobate-based ILs. As far as we know, this is the first example of the highly selective epoxidation of olefins and allylic alcohols by using supramolecular ILs as catalysts.

1. Introduction

The epoxidation of olefins and allylic alcohols plays an essential role in industrial and synthetic chemistry [1–3]. Many high value-added products such as surfactants, perfumes and epoxy resins are manufactured from epoxides [4]. However, peracids and hazardous solvents are usually involved in epoxidation reaction, which are expensive and environmentally harmful [5]. Comparatively, hydrogen peroxide is possibly the best oxidant except for oxygen in consideration of environment and economy considering that water is the sole product along with H₂O₂ consumption [6].

As for olefin epoxidation reactions, a microporous titanium silicate zeolite (TS-1) exhibits extensive application in epoxidizing light alkenes with hydrogen peroxide [7]. Nevertheless, long-chain olefins cannot facilely contact the reactive centers due to the small pore sizes of TS-1. In addition, the active species of TS-1 are liable to leach in the course of epoxidation with H₂O₂ as oxidant [8]. Meanwhile, various homogeneous transition-metal complexes have been applied to highly efficient

olefin epoxidation [9]. For example, some homogeneous tungsten complexes afforded much better catalytic activity than heterogeneous analogues in the epoxidation of alkenes [10,11]. Besides, the complexes of early transition metals, especially molybdenum complexes (oxomolybdenum species), have also shown good catalytic activity and selectivity [12,13]. However, the homogeneous complex catalysts are confronted with challenges including the oxidative decomposition under reaction conditions and the difficult separation and recovery, greatly limiting their applications. On the other hand, the simple loading of the tungsten-based precursor onto porous siliceous molecular sieves typically causes uneven surface WO₃ domains, which is thus prone to further aggregation, resulting in activity loss and scarce robustness [14]. Although much efforts have been made to grafting the complexes of transition metals to porous solid materials by strong covalent linkage, the inherent catalytic activity of metal complexes is normally reduced because of the adverse interactions of active sites with non-uniform solid surfaces [15,16]. Hence, the development of highly active and recoverable catalysts is fairly promising, which is also in line with the

* Corresponding authors.

E-mail addresses: yfyao@phy.ecnu.edu.cn (Y. Yao), houshenshan@ecust.edu.cn (Z. Hou).

<https://doi.org/10.1016/j.mcat.2020.111342>

Received 30 September 2020; Received in revised form 1 December 2020; Accepted 7 December 2020

Available online 28 December 2020

2468-8231/© 2020 Elsevier B.V. All rights reserved.

requirements of green chemistry.

Niobium-based compounds can be extensively studied as the catalytic materials [17,18]. For examples, Nb-silicates offer more advantages with respect to hydrolytic stability as compared with that of V and Mo catalysts [19]. Especially, as potential oxygen donors, niobium complexes have received increasing attention in oxidation reaction recently [20]. The previous studies have confirmed that the peroxo niobium complexes are able to release active oxygen either chemically or on irradiation, thus participating in oxidation of various organic substrates [21].

Ionic liquid (IL) has been represented as a research hotspot recently owing to their distinctive natures containing a wide liquid range, non-volatility, ionicity and strong polarity [22–24]. These specific properties of ILs have opened up their applications in the industry as reaction solvents, catalysts, electrolytes, sensors, enzyme stabilizers [25,26]. The structures and properties of ILs can be easily designed and adjusted via varying their cations and inorganic anions. Currently, a great deal of functionalized ILs have been investigated, providing a promising methodology to synthesize catalysts with high performance and excellent recyclability [27]. As a subset of functionalized ILs, polyoxometallate anion-based ILs (POM-ILs) have been achieved and employed in acid-catalysis and oxidative reaction with excellent catalytic activity and reusability [28,29]. There is no doubt that the appearance of the functionalized ILs will assure the ILs with different particular capabilities, promoting more sustainable and reasonable development of ILs [30,31]. In our previous research, a series of peroxoniobate (peroxotantalate)-based ILs have been utilized in epoxidizing olefins and allylic alcohols [32,33]. These ILs catalysts showed huge advantages in separation and recycling and demonstrated better performance in catalytic epoxidation compared to tungsten-containing catalysts. However, the preparation of these ILs normally needs tedious procedures such as neutralization, ionic exchange and solvent removal etc., which contains time-consuming multiple operations and might bring impurities in ILs.

As a branch of noncovalent interplay and supramolecular chemistry, host-guest interaction exists extensively between metal cations and macrocyclic ethers [34,35]. In recent years, crown ethers have drawn growing interest because they are capable of forming complexes selectively with ionic species by host-guest interaction [36]. In the previous studies, a crown ether complex cation ILs were employed for various carbon-carbon bond-forming reactions, including Michael addition, Heck reaction and Henry reaction [37]. It indicated that these ILs can be recycled for many times without significant deactivation. Sequentially, the numerous deep eutectic solvents have been developed based on host-guest interactions [38,39]. However, up to now the specific ILs formed by the host-guest interactions have seldom been reported for catalysis, let alone oxidation reaction.

According to our previous work, organic acid-modified peroxoniobate ILs had high reactivity toward the epoxidation reaction [33]. However, the synthesis of the specific ILs was rather tedious due to multiple steps. As a continuous effort to optimize the catalytic application of the ILs, in this work we have developed a novel type of ILs formed by supramolecular interactions. The supramolecular ILs can be obtained by a direct mixing of CE with the $\text{NH}_4\text{-Nb}((\text{NH}_4)_3[\text{Nb}(\text{O}_2)_4])$ with the certain molar ratio in methanol. Afterwards, the methanol was evaporated under the vacuum to generate the ILs without any by-products, which was a much simpler approach in comparison to that of the previous work [33,40]. The supramolecular complexation of CE and $\text{NH}_4\text{-Nb}$ has been proved by FT-IR spectra, differential scanning calorimetry (DSC) and conductivity measurement etc. Notably, the easily available ILs demonstrated the excellent catalytic performance for the epoxidation under very mild conditions.

2. Experimental

2.1. Materials

18-crown-6 (CE, $\text{C}_{12}\text{H}_{24}\text{O}_6$, 98 wt.%) was provided by Bide Pharmatech Ltd. Potassium hydroxide (KOH) and Hydrogen peroxide (H_2O_2 , 30 wt.%) were supplied by Shanghai Titan Scientific Co., Ltd. Niobium pentaoxide (Nb_2O_5), ammonium hydroxide ($\text{NH}_3\cdot\text{H}_2\text{O}$, AR) and methanol (CH_3OH , AR) were purchased from Aladdin. Glycolic acid (GLY, $\text{C}_2\text{H}_4\text{O}_3$, 98 wt.%) was supplied by TCI (Shanghai) Development Co., Ltd.

2.2. Catalyst characterization

The procedures for catalyst characterization can be found in Supporting Information.

2.3. Catalyst preparation

2.3.1. Synthesis of $(\text{NH}_4)_3[\text{Nb}(\text{O}_2)_4]$

At first, $\text{Nb}_2\text{O}_5\cdot n\text{H}_2\text{O}$ was prepared by sintering KOH and Nb_2O_5 in a molar ratio of 10 ($n_{\text{KOH}/\text{Nb}_2\text{O}_5} = 10$) at 550 °C for 6 h [41]. Subsequently, the mixture was dissolved in water and acidified by acetic acid with pH reaching to 4. The white precipitate was obtained by filtration and washed thoroughly, followed by drying at 60 °C for 1 h. Then $\text{NH}_4\text{-Nb}((\text{NH}_4)_3[\text{Nb}(\text{O}_2)_4])$ was obtained from the reaction of the $\text{Nb}_2\text{O}_5\cdot n\text{H}_2\text{O}$ and H_2O_2 , adjusting pH around 10 with $\text{NH}_3\cdot\text{H}_2\text{O}$ until the solution became clear. Ethanol was poured into the clear solution to precipitate the $\text{NH}_4\text{-Nb}((\text{NH}_4)_3[\text{Nb}(\text{O}_2)_4])$ as a white powder [42]. Anal. Calcd for $\text{NH}_4\text{-Nb}$ (274.97): Nb, 33.8. Found: Nb, 33.1. Number of peroxide bonds: 3.6.

2.3.2. Preparation of $(\text{CE})_6(\text{NH}_4)_4[\text{Nb}_2\text{O}_4(\mu\text{-O})(\eta^2\text{-O}_2)_2](\text{CE-1})$

The IL (CE-1) was obtained according to the following procedure. Briefly, CE (0.79 g, 3 mmol) and $\text{NH}_4\text{-Nb}$ (0.27 g, 1 mmol) (CE/Nb = 3:1) were stirred in 10 mL of methanol at 60 °C for 24 h. The clear solution was rotary evaporated to obtain the light yellow viscous liquid as $(\text{CE})_6(\text{NH}_4)_4[\text{Nb}_2\text{O}_4(\mu\text{-O})(\eta^2\text{-O}_2)_2]$, designated as CE-1 (Fig. S1). ^1H NMR (400 MHz, D_2O): 3.33 (s, 0.12 H), 3.67 (s, 6.15 H), 4.79 (s, 1 H). ^{13}C NMR (100 MHz, D_2O): δ 70.21, 49.50 (Fig. S2). Anal. Calcd for $\text{C}_{72}\text{H}_{160}\text{N}_4\text{Nb}_2\text{O}_{45}$ (1987.87): C, 43.46; H, 8.05; N, 2.81; Nb, 9.35. Found: C, 42.70; H, 7.70; N, 2.50; Nb, 9.20. Number of peroxide bonds: 1.5 per Nb atom.

2.3.3. Preparation of $(\text{CE})_6(\text{NH}_4)_4[\text{Nb}_2\text{O}_4(\mu\text{-O})(\text{GLY})_2](\text{CE-2})$

The preparation of CE-2 was similar to that of CE-1. Firstly, CE (0.79 g, 3 mmol) was dissolved in 10 mL of methanol and $\text{NH}_4\text{-Nb}$ (0.27 g, 1 mmol) was then added to the above solution with the molar ratio of CE/Nb = 3:1. The resulting mixture was stirred at 60 °C for 24 h until it became a clear solution. Next, GLY (0.08 g, 1 mmol) was dissolved in 2 mL of methanol and added dropwise to the above solution. The mixture was then agitated intensely at 40 °C for another 12 h, and the solvent was removed with a rotary evaporator. The resultant IL was placed under vacuum at 40 °C to obtain yellow viscous liquid $((\text{CE})_6(\text{NH}_4)_4[\text{Nb}_2\text{O}_4(\mu\text{-O})(\text{GLY})_2])$, designated as CE-2 (Fig. S1). ^1H NMR (400 MHz, D_2O): 3.34 (s, 2 H), 3.68 (s, 44 H), δ 3.98 (s, 1 H), 4.79 (s, 8 H). ^{13}C NMR (100 MHz, D_2O): δ 179.84, 171.03, 72.37, 70.20, 61.71, 49.50 (Fig. S3). Anal. Calcd for $\text{C}_{76}\text{H}_{164}\text{N}_4\text{Nb}_2\text{O}_{47}$ (2071.94): C, 44.01; H, 7.91; N, 2.70; Nb, 8.98. Found: C, 42.27; H, 7.48; N, 2.66; Nb, 8.89. Number of peroxide bonds: 0.5 per Nb atom.

For the sake of comparison, CE-2a and CE-2b were prepared in a similar way but 2 mmol CE (CE/Nb = 2) or 4 mmol CE (CE/Nb = 4) was charged to 10 mL of methanol solution of $\text{NH}_4\text{-Nb}$, respectively, followed by adding GLY (0.08 g, 1 mmol). The resultant solution was agitated at 40 °C for 12 h, and then the solvent was removed to afford CE-2a and CE-2b, respectively. CE-2a $((\text{CE})_4(\text{NH}_4)_4[\text{Nb}_2\text{O}_4(\mu\text{-O})$

(GLY)₂): Anal. Calcd for C₅₂H₁₁₆N₄Nb₂O₃₅ (1542.55): C, 40.45; H, 7.52; N, 3.63; Nb, 12.06. Found: C, 39.88; H, 7.39; N, 3.52; Nb, 11.29. CE-2b ((CE)₈(NH₄)₄[Nb₂O₄(μ-O)(GLY)₂]): Anal. Calcd for C₁₀₀H₂₁₂N₄Nb₂O₅₉ (2599.18): C, 46.17; H, 8.16; N, 2.15; Nb, 7.16. Found: C, 45.45; H, 7.89; N, 2.05; Nb, 7.05. FT-IR spectra of both CE-2a and CE-2b were given in Fig. S4.

2.4. Typical method for the epoxidation

Catalysts (0.01 mmol), olefins (1 mmol), an internal standard (dodecane) and 30 % aqueous H₂O₂ (1 mmol) were dissolved in CH₃OH (2 mL) and then charged into a 25 mL Schlenk flask. The reaction mixture was agitated intensely at 50 °C for different time. After reaction, the reaction mixture was extracted with cyclohexane at least three times, which was also monitored by gas chromatography (GC). In catalyst recycling, after extraction with cyclohexane the remaining catalyst was evaporated to dryness under vacuum at 40 °C and could be used for the next run.

2.5. Catalytic kinetics of epoxidation

The method of studying reaction kinetic for the epoxidation reaction by using the supramolecular ILs is displayed as follows. Cyclooctene (1 mmol), catalyst (0.01 mmol), an internal standard (dodecane) and 30 % aqueous H₂O₂ (1 mmol) were dissolved in CH₃OH (2 mL), and then the mixture was agitated and heated to designed temperature (303–333 K) and time. The reaction process was monitored by GC and reaction rates were obtained accordingly under low conversions of cyclooctene (<20 %). Then the rate constants were calculated at the different temperatures based on initial rate method [43]. The activation energy was achieved by following Arrhenius equation.

3. Results and discussion

3.1. Catalyst characterization

The IL catalysts (such as CE-1 and CE-2) were all yellow and exhibited the common features of ILs like a viscous liquid around ambient temperature and non-volatility. Additionally, they were immiscible with low-polarity or non-polarity solvents (such as alkane, ethyl acetate, toluene, etc.), but fully miscible with polar solvents (H₂O, CH₃OH, CH₃CH₂OH, CH₃CN etc.) (Table 1).

Based on the elemental analysis, potential difference titration of Ce³⁺/Ce⁴⁺ and other characterization (following section), it indicated that anions of the ILs existed in the form of the dimeric structure likely owing to the supramolecular complexation between CE and ammonium cations. The dimeric structure has been depicted in Fig. 1.

The host-guest interaction in the specific ILs was firstly investigated by DSC. As shown in Fig. 2 (Left), the melting point of the sole CE is around 43.34 °C and the melting point of the ionic compound NH₄-Nb could be very high and not available because it was labile to decompose prior to melting (Fig. 2, left). Comparatively, the melting point of two ILs

Table 1

The physico-chemical properties of the NH₄-Nb and the IL catalysts.

Samples	M.p./ °C	States	Peroxy- bond/Nb	Solubility ^a			
				H ₂ O	CH ₃ OH	AcOEt	PhCH ₃
NH ₄ -Nb	N.D. ^b	White powder	3.6	√	×	×	×
CE-1	36.30	Yellow liquid	1.5	√	√	×	×
CE-2	34.08	Yellow liquid	0.5	√	√	×	×

^a √: soluble, ×: insoluble.

^b N.D: Not determined.

like CE-1 and CE-2 were determined as 36.30 °C and 34.08 °C respectively, indicated that the melting point was obviously lower than that of a sole CE (Fig. 2, left). The reduced melting points actually reflected that the hydrogens of the NH₄⁺ might interact with the oxygens of CE by hydrogen bonding, and NH₄⁺ could diffuse into the flexible holes of the CE considering that the radius of ammonium was close to the size of the cavity of CE [44], leading to a decreased coulomb interaction due to the distribution of positive and negative charge [45,46]. The small peak around 47 °C (Fig. 2c, left) could be assigned to a minor dimer form besides the structure of CE-1 due to the labile peroxy group. Subsequently, the ILs with the different molar ratios of CE/NH₄-Nb were also prepared and characterized by DSC. It was observed visually that if the molar ratio of CE/Nb decreased to 1:1, the reaction between CE and NH₄-Nb in methanol was unable to lead to the clear solution, indicating that the supermolecular complexes were not formed under this condition. However, the molar ratio of CE/Nb = 2:1 (CE-2a) and 4:1 (CE-2b) would result in the formation of the supermolecular ILs. Next, the DSC curves of CE-2a and CE-2b were also conducted and shown in Fig. S5. It indicated that the molar ratio of CE/Nb has a subtle influence on the melting point of supermolecular ILs likely due to a symmetrical structure of CE. It should be noted that if the molar ratio of CE/Nb was increased up to 4:1 (CE-2b), the resulting IL actually contained a part of free CE, whose melting point (42.88 °C) was very close to that of the sole CE (43.34 °C) (Fig. 2 vs Fig. S5c). Consequently, a 3:1 M ratio of CE/Nb has been chosen as the optimal ratio in this work.

Next, these synthesized ILs were characterized with FT-IR spectroscopy. As can be seen in Fig. 2 (right), the band of CE at approximately 2887 cm⁻¹ arose from the vibration of C-H and the band near 1112 cm⁻¹ was belong to ν(C-O) [47]. In addition, the band in NH₄-Nb near 3169 cm⁻¹ was related to the vibration of N-H and the band at 815 cm⁻¹ was characteristic for ν(O-O) [48]. However, some of the peaks showed obvious shifts after CE was added to the original NH₄-Nb, forming the specific ILs (Fig. 2c and 2d, right). The band near 815 cm⁻¹ attributing to ν(O-O) of NH₄-Nb moved from 815 cm⁻¹ to ca. 858 cm⁻¹, revealing the existence of only one sort of peroxy bond. Obviously, a blue shift of N-H of ammonium ion was observed as the ILs was derived from NH₄-Nb (Fig. 2b vs 2c and 2d, right), which indicated the hydrogen bonding interaction between CE and ammonium ion. Meanwhile, the host-guest interaction can also be evidenced by the shape of the characteristic peak around 3540 cm⁻¹ corresponding to the ν(C-H) of crown, which became broader after forming the specific ILs, indicating that NH₄⁺ was likely bonded in the hole of CE, and thus the CE framework was affected by supramolecular interaction as well [49]. Additionally, the bands near 590 and 536 cm⁻¹ were assigned to vibration of Nb-O in ILs [50]. The existence of the stretching of Nb-O-Nb bridge near 836 cm⁻¹ evidenced that the peroxoniobate anion could be formed as dimer rather than mononuclear form [51]. Moreover, as compared to the band of peroxy bonds in CE-1 (Fig. 2c, right), the intensity of the band around 858 cm⁻¹ (O-O species) became weaker in organic acid coordinated crown-based ILs, suggesting the substitution of peroxy bonds by carboxylate ligands (Fig. 1). Meanwhile, the band near 1654 cm⁻¹ could be assigned to the vibration of COO- coordinating with the niobium atom [33]. The result was also highly consistent with the result of the potential difference titration of Ce³⁺/Ce⁴⁺ (Table 1). It can be seen that in spite of the different CE/Nb, the FT-IR spectra of CE-2a and CE-2b were close to that of CE-2 (Fig. S4 vs Fig. 2d, right), demonstrating that their anion structures were very similar to each other.

Next, the conductivity of CE and the ILs in the aqueous solution was determined as well. It was known that the conductivity was closely relevant to ionic diffusion rate [52]. As shown in Fig. 3, the conductivity was approximately linear to the concentration of Nb (C_{Nb}) under low concentrations (0–2 mmol·L⁻¹). Notably, the conductivity of NH₄-Nb was much greater than that of the derived ILs in the aqueous solution. The conductivity (σ) is positively correlated with the ionic diffusion coefficient according to the Nernst-Einstein Eq. (1) [53]:

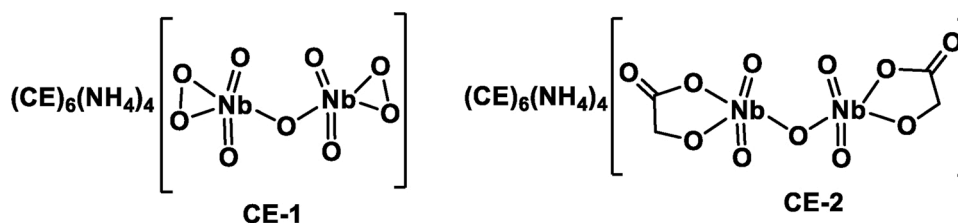
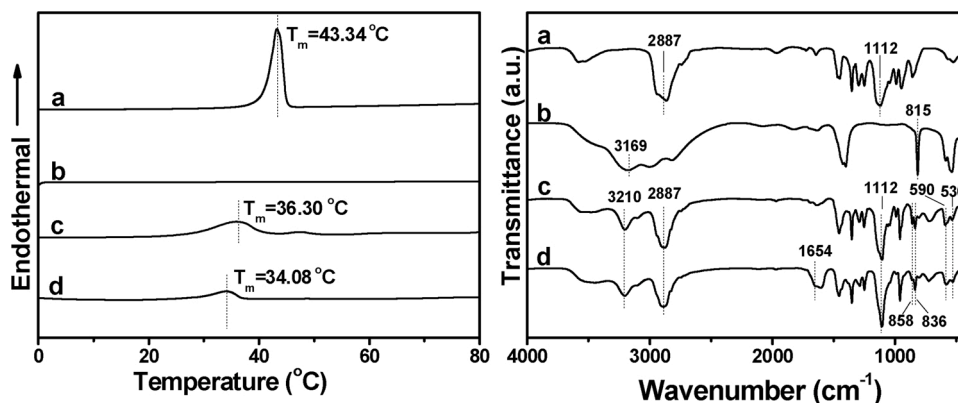
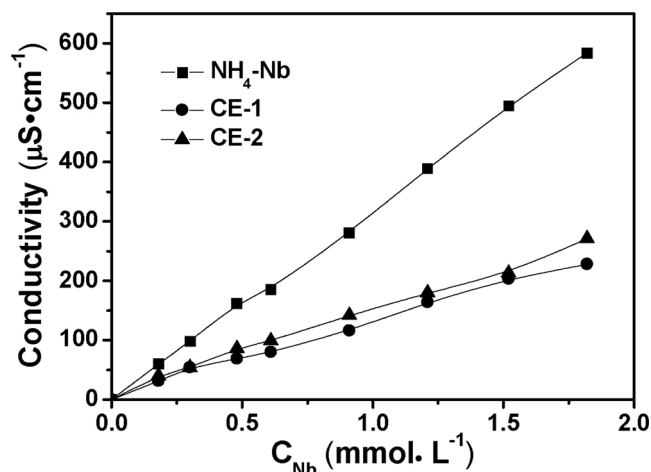


Fig. 1. Proposed dimer structure of CE-1 and CE-2.

Fig. 2. DSC patterns (left) and FT-IR spectra (right) of (a) CE, (b) NH₄-Nb, (c) CE-1, and (d) CE-2.Fig. 3. The conductivity as function of the C_{Nb} at 25 °C, where C_{Nb} represented the molar concentration of Nb in H₂O.

$$\sigma = \frac{F^2}{RT} \alpha c (D^+ + D^-) \quad (1)$$

where α is degree of dissociation, σ is conductivity of compound, c represents molar concentration of compound, D^+ and D^- are the diffusion coefficients of ions, F is Faraday number, R is gas constant, and T is absolute temperature. The results from the conductivity measurement implied that the diffusion coefficient of ions in derived ILs was much smaller than that of NH₄-Nb (Fig. 3). It has been reported that the diffusion coefficient of ions was highly dependent on the size and functional group of molecules [54,55]. The obvious reduction of the diffusion coefficient indicated the supramolecular association of the ammonium peroxy niobate with CE, leading to formation of the specific ILs.

The as-synthesized ILs were also characterized by Raman spectroscopy. As shown in Fig. 4a (CE-1), the band near 580 cm⁻¹ was attributed

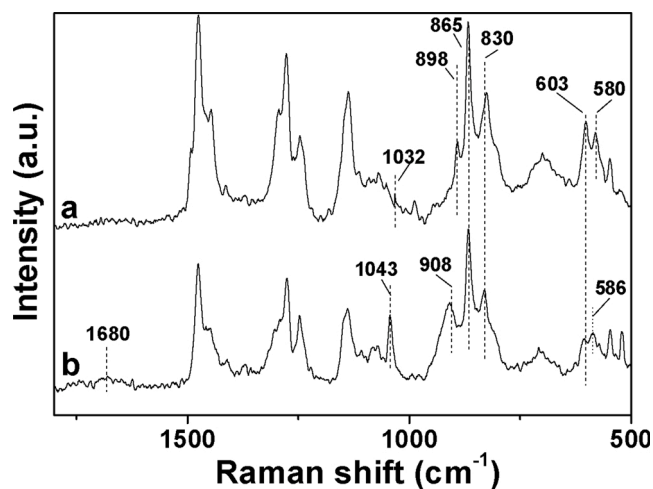


Fig. 4. Raman spectra of (a) CE-1, (b) CE-2.

to $\nu_s(\text{Nb}(\text{O}_2))$ and the band at 603 cm⁻¹ was assigned to the vibration of Nb-O [56]. Besides, the band around 830 cm⁻¹ was attributing to the stretching of the Nb-O-Nb and the band at 865 cm⁻¹ was related to vibration of O-O [48]. Additionally, the band around 898 cm⁻¹ which resulted from $\nu(\text{Nb}=\text{O})$ was inactive in FT-IR spectroscopy but active in Raman spectroscopy, showing a high symmetry in structure of the IL. Moreover, the band at 1032 cm⁻¹ was attributed to $\nu(\text{C}-\text{O})$. For GLY coordinated IL (CE-2), the band assigned to $\nu_s(\text{Nb}(\text{O}_2))$ shifted from the former 580 cm⁻¹ to 586 cm⁻¹ and the intensity became weaker (Fig. 4a vs 4b), indicating that the peroxy band in CE-1 was replaced by the carboxylato ligands. The band attributed to $\nu(\text{Nb}=\text{O})$ shifted from 898 cm⁻¹ to 908 cm⁻¹ and the band at 1043 cm⁻¹ was assigned to $\nu(\text{C}-\text{O})$. Meantime, the band near 1680 cm⁻¹ was related to $\nu(\text{COO}^-)$ which was coordinated with niobium atom by forming five-membered ring. The results indicated that both carboxylato group and neighboring hydroxyl group in GLY molecule were involved in generating complexes [57].

These results are in line with the structure of ILs as shown in Fig. 1

The thermogravimetric analysis (TGA) of the ILs was conducted sequentially. As shown in Fig. 5, the obvious weight losses of approximately 89.8 % and 86.5 % were seen between 40 and 800 °C, which could be assigned to the decay of organic cations and carboxylate group in anion species. The weight loss at the beginning could be due to adsorbed water on ILs. The weight of ILs started to decrease sharply at approximately 200 °C, confirming that thermal stability of the specific ILs was almost identical to that of these conventional ILs.

The matrix-assisted laser desorption and ionization time-of-flight mass spectrometry (MALDI-TOF) was thereafter utilized to investigate the dimer structure of ILs dissolved in water in the negative mode (Fig. S6a and S6b). The peaks of CE-1 dominantly existed at 516.9 *m/z*, 671.9 *m/z*, 687.9 *m/z* and 861.0 *m/z*, and the peaks of CE-2 presented at 500.9 *m/z*, 558.9 *m/z*, 672.0 *m/z*, 688.0 *m/z* and 861.1 *m/z*, respectively. The other unlabeled peaks are belonging to those of matrix molecules (CHCA). The other probable structures were displayed in Table S1, which revealed that CE-1 and CE-2 indeed existed in the form of the dimeric structure rather than mononuclear structure. The results of MALDI-TOF were then in line with those of elemental analysis, FT-IR and Raman spectra.

3.2. H₂O₂-induced structure transformation of peroxoniobate anion

It is crucial to clarify how the specific IL anions evolved during the epoxidation. Next, the transformation of peroxoniobate anion in the ILs was determined by ⁹³Nb NMR spectra. As shown in Fig. 6a, a mononuclear NH₄-Nb complex exhibited a resonance signal at -1522 ppm, which was in well agreement with that of our previous result [32]. When the NH₄-Nb was complexed with CE, the resulting CE-1 displayed a peak around -1160 ppm, indicating that the supramolecular interaction indeed has a considerable effect on the structure of peroxoniobate anion (Fig. 6b). Additionally, on coordinating with GLY, the chemical shift was further moved to low field and the signal shifted to -1000 ppm (Fig. 6c). This was due to a decrease of electron density around niobium atom when the peroxo bond was substituted by GLY acting as electron-withdrawing groups [58]. Especially, the presence of only one peak in CE-1 or CE-2 in ⁹³Nb NMR indicated that the binuclear Nb-O-Nb sites in the supramolecular ILs might exist in the same chemical environment. In combination with the characterization of FT-IR, Raman, MALDI-TOF and ⁹³Nb NMR, the evidences suggest that CE-1 and CE-2 exhibit as highly symmetric dimeric structure (Fig. 1).

It was observed visually that when the present ILs were mixed with H₂O₂, an obvious exothermic phenomenon occurred. According to the experimental observation, the peroxoniobate anion could undergo the transformation of structure under action of H₂O₂. To investigate evolution of anion structure, CE-2 (0.4 mmol) was dissolved in methanol (2 mL), and then H₂O₂ (4 mmol) was dropped into the methanol solution and agitated continuously for 0.5 h at 273 K. The diethyl ether was immediately added to solution and then the sediment of the oxidizing

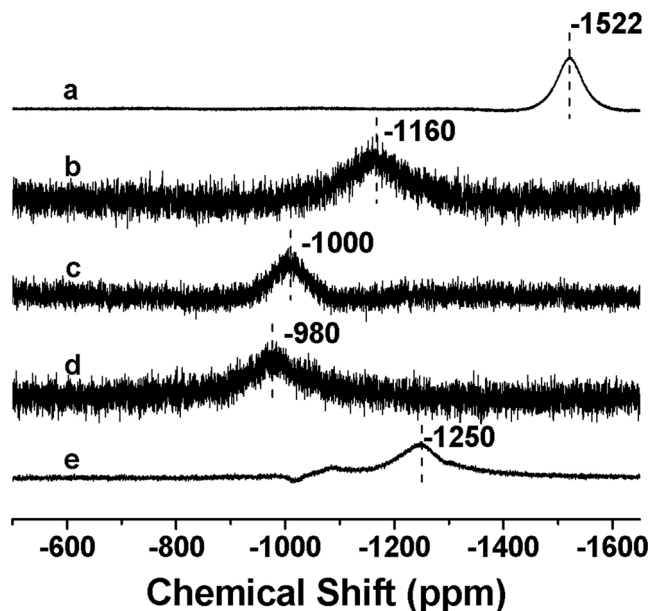


Fig. 6. ⁹³Nb NMR spectra of different samples: (a) NH₄-Nb, (b) CE-1, (c) CE-2, (d) reused CE-2 and (e) CE-2 in H₂O₂.

Nb species was collected, which was washed with diethyl ether and was dried with cold air to get the oxidizing species sequentially. It was seen that the resulting oxidizing species owned a resonance signal at -1250 ppm in D₂O (Fig. 6e), which appeared in higher field compared to other peroxoniobium species expect for NH₄-Nb, implying the different chemical environment around niobium in oxidizing peroxoniobium species (Fig. 6e). The resonance signal shifting to high field meant more numbers of peroxo groups around niobium sites, which revealed that the peroxoniobate anion was further oxidized in the presence of H₂O₂. Additionally, Raman spectra of the oxidizing peroxoniobium species demonstrated the same phenomenon. As shown in Fig. 7, there was a great difference in the characteristic peaks between the parent CE-2 and the oxidizing species (Fig. 7 vs 3b). The intensity of the bands at approximately 865 cm⁻¹ and 581 cm⁻¹ became stronger respectively, which were attributed to ν(O—O) and ν_s(Nb(O₂)). Besides, the band at 908 cm⁻¹ (vibration of Nb = O species) disappeared in the oxidizing species of the CE-2, revealing that the evolution from Nb = O to niobium peroxo groups were actually reversible in the course of reaction condition. Meantime, the band related to vibration of Nb-O moved from 603 cm⁻¹ to 613 cm⁻¹, reflecting that Nb = O and Nb-O bonds were highly dependent on each other.

Further on, the peroxo number of the oxidizing form of CE-2 was measured via potential difference titration of Ce³⁺/Ce⁴⁺. The number of peroxo bonds was almost two per Nb atom in the dimer, indicating the

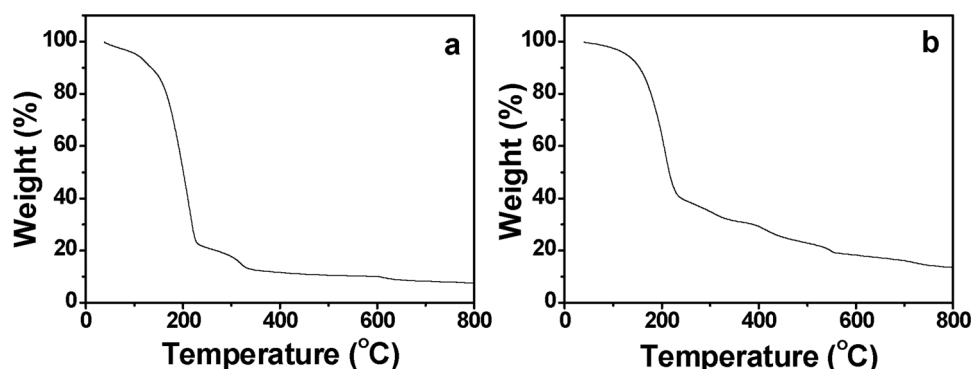


Fig. 5. TGA patterns of the crown ionic liquids: (a) CE-1; (b) CE-2.

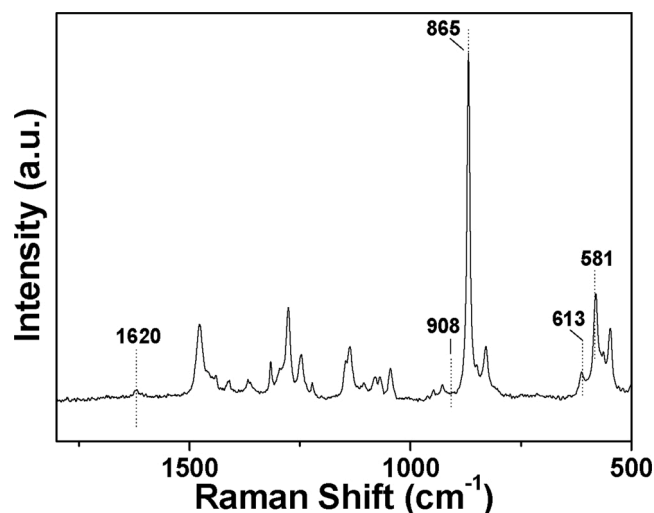


Fig. 7. Raman spectra of the oxidizing species of CE-2.

oxidizing Nb species contained nearly four peroxy bonds, which is in accordance to the variation trend of ^{93}Nb NMR.

3.3. Catalytic performance

The cyclooctene was firstly chosen as model substrate for the epoxidation with H_2O_2 by using the IL catalysts at 50°C with methanol as solvent. As displayed in Table 2, the epoxidation might hardly proceed in the absence of catalysts (Table 2, entry 1), implying that only the H_2O_2 cannot epoxidize cyclooctene. CE also afforded poor activity in epoxidizing olefins (Table 2, entry 2). Obviously, GLY itself hardly epoxidized olefins (Table 2, entry 3), implying that the organic peroxy acid couldn't be active species for the epoxidation under the present condition. Moreover, $\text{NH}_4\text{-Nb}$ was also inactive for epoxidation reaction (Table 2, entry 4). The $\text{NH}_4\text{-Nb}$ had a very poor solubility in methanol and the reaction mixture showed a clear solid-liquid biphasic in the course of the reaction. However, the IL CE-1 was dissolved in the methanol and remained a homogeneous phase, and it showed much better performance than $\text{NH}_4\text{-Nb}$ (Table 2, entries 4 vs 5). These results confirmed that catalytic active sites might result from the part of peroxoniobate anions and the supramolecular complexation of the ammonium ion (NH_4^+) with the CE led to better performance of the epoxidation reaction because of the better miscibility of the catalyst in the methanol [59,60]. Next, the effect of the anion structure on catalytic performance

Table 2
Epoxidation of cyclooctene with various catalysts^a.

Entries	Catalysts	Additives	Con. (%) ^b
1	none	none	1
2	CE	none	1
3	Glycolic acid	none	1
4	$\text{NH}_4\text{-Nb}$	none	2
5	CE-1	none	60
6	CE-2	none	99
7 ^c	CE-1	acetic acid	63
8 ^c	CE-1	3-hydroxypropionic acid	62
9 ^c	CE-1	oxalic acid	40
10 ^c	CE-1	lactic acid	83
11 ^c	CE-1	glycolic acid	98
12	CE-2a	none	93
13	CE-2b	none	98

^a Reaction conditions: Cyclooctene (1 mmol), H_2O_2 (1 mmol), 2 mL of CH_3OH , IL catalyst (0.01 mmol), 50°C , 3 h. Epoxide was detected as a sole product in all reaction.

^b The conversion was obtained by GC with dodecane as an internal standard.

^c 0.02 mmol of additive was used.

has been investigated. An interesting phenomenon was that epoxidation reaction proceeded even more efficiently when CE-1 was coordinated with GLY. The resulting IL CE-2 exhibited an excellent catalytic performance (Table 2, entry 6). This was because that organic ligand (GLY) acting as an electro-withdrawing group tended to decrease the electron density of Nb anion. The resulting electron-poor reaction sites ($\text{O}-\text{O}$) was more prone to react with $\text{C}=\text{C}$ double bond due to electrophilic addition mechanism of the epoxidation process [61,62].

It has been found that introduction of 3-hydroxypropionic acid and acetic acid did not improve the catalytic activity at all, affording the almost same performance as parent IL (Table 2, entries 5, 7 and 8). Besides, when oxalic acid was added to CE-1, the conversion dropped down sharply due to too strong coordination interaction between oxalic acid and niobium sites (Table 2, entry 9), likely preventing the substrate molecules accessible to the reaction sites. However, lactic acid was proved to be a more effective additive than that of oxalic acid (Table 2, entry 10). Notably, the GLY was the best additive, and almost full conversion of cyclooctene could be achieved under the identical condition (Table 2, entry 11). The results suggested that only α -hydroxy carboxylic acid had a favorable influence on epoxidation reaction. Additionally, it should be noticed that the molar ratio of CE/Nb had a subtle effect on catalytic activity (Table 2, entries 6, 12 and 13) when specific ILs were generated via the NH_4^+ complexation with crown ether ring, which can be further confirmed via the time profile of the epoxidation using CE-2, CE-2a and CE-2b as catalysts (Fig. S7). CE-2 and CE-2b could show a slightly better activity, as compared with CE-2a, implying that increasing amount of CE could be beneficial to interaction between substrate and active centers due to appropriate hydrophobicity.

The effect of the solvents was sequentially investigated for epoxidizing cyclooctene with CE-2 as a catalyst. As shown in Table S2, the catalytic activity is very poor under solvent-free conditions, and the poor activity was also observed in ethyl acetate and dichloromethane likely owing to biphasic state under the conditions used. (Table S2, entries 1–3). However, the conversions of cyclooctene can reach up to 43 %, 82 %, 99 % in acetonitrile, ethanol and methanol, respectively (Table S2, entries 4–6). These data suggested that the strongly polar protic solvents, especially methanol could enhance the epoxidation reaction (Table S1, entries 4–6). It has been demonstrated from the previous work that the proton in the solvent participated in the formation of active intermediates via hydrogen bonding, which were favorable for the epoxidation of substrates [63].

A radical mechanism has been suggested in oxidation reactions for niobium-containing catalysts [64,65]. In this work, butylated hydroxytoluene (BHT) was used as a free radical trapper to investigate possible reaction mechanism, (Fig. S8). After reaction started for some time, the homogeneous mixture was separated into two parts. The one part continued to stir for reaction, and the second part was added 0.5 mmol BHT. Both of parts were subjected to GC analysis consecutively. As displayed in Fig. S8, the introduction of BHT had no any effect on the epoxidation reaction, demonstrating clearly that the epoxidation reaction occurred by catalytic mechanism instead of radical approach [66]. In addition, the EPR spectrum of the $\text{DMPO}/\cdot\text{OH}$ adduct kept silent under the reaction condition (Fig. S9), suggesting that $\cdot\text{OH}$ radical could be not possibly involved in the oxidation reaction, in line with that of the above activity tests using BHT as free radical trapper.

3.4. Kinetic studies

The cyclooctene has been selected as model substrate for the following kinetic investigation. With respect to the previous investigation of other groups and our work [32,33,43], the epoxidation of alkenes displayed the first-order dependence on the concentration of olefins and the zero-order dependence on H_2O_2 at low concentrations, indicating that the concentration of olefins rather than hydrogen peroxide could be responsible for the rate-limiting transition state. First, the influence of dosage of catalysts and stirring speeds on the reaction rate was studied

to exclude limitations of diffusion (Fig. S10). Next, the dependence of reaction rate of cyclooctene on temperature (Arrhenius plots, 303–333 K) was examined with different ILs. The rate constants were obtained at low conversions (<20 %) on the basis of initial rate method. As can be seen in Fig. 8, the linearity of Arrhenius plots was determined and activation energy was calculated on the basis of the pseudo-first-order kinetics pattern. It indicated that activation energy of CE-2 was only 29.81 kJ mol⁻¹ which was below that of CE-1 ($E_a = 58.99$ kJ mol⁻¹). The activation energy of the current ILs was also below that of the previous report, of which the activation energies were around 50–100 kJ mol⁻¹ [67]. Actually, the activation energy of the current IL CE-2 was very close to that of carboxylic acid-modified peroxoniobate-based ILs [33], confirming that the present CE-2 was also a superior catalyst for epoxidation, but it was much easily available just via a supramolecular interaction, as compared with the peroxoniobate-based IL.

3.5. Substrate scope and recyclability

Subsequently, the activity tests were performed to investigate the range of the substrates. As shown in Table 3, various olefins and allylic alcohols were epoxidized into the corresponding epoxides with only 1 equiv of H₂O₂ with CE-2. A conversion in the range of 21–99 % was gained for epoxidation of cyclic olefins and chain olefins using methanol as the solvent (Table 3, entries 1–7). The epoxidation of cyclooctene showed better reactivity and selectivity in comparison to cyclohexene in the epoxidation of which the by-products were cyclohexane-1,2-diol and 2-methoxycyclohexanol detected by GC-MS (Table 3, entry 1 vs 2). The 2-cyclohexen-1-ol and cyclohexanone was not detected in the products, implying that a single electron transfer approach was not included in the epoxidation. Overall, the performance of the epoxidation of cyclic olefins was better than that of chain olefins. Interestingly, the conversion of trans-2-octene was obtained at approximately 21 %, which was lower than that of cis-2-octene (Table 3, entry 4 vs 5). The result suggested that steric hindrance around C=C could have an important influence on the

epoxidation reactivity, demonstrating that the process did not proceed by free radical mechanism. Moreover, the propylene can likewise be epoxidized to propylene oxide selectively under the present conditions, and the yield was around 32 % under 1.5 MPa of propylene pressure, providing a promising result for possible application. In addition, the IL CE-2 also had good catalytic activity and selectivity in the epoxidation of allylic alcohols (Table 3, entries 8–12). For long-chain allylic alcohols, methanol was needed to achieve higher reactivity and selectivity (Table 3, entries 9 and 12). Moreover, the oxidation of geraniol was regioselective because that hydroxyl groups in geraniol can be coordinated with Nb anion [32], and the main products were 2,3-epoxygeraniol. Nevertheless, when an electron-withdrawing group was around C=C, a low reactivity for the epoxidation was obtained. The conversion of allyl methyl ether was low in comparison to other allylic alcohols, which was due to electrophilic addition mechanism of epoxidation (Table 3, entry 13). Besides, the hydroxyl group adjacent to the double bond could play a key role in bring C=C bonds close to the peroxy oxygen, and facilitating the transfer of oxygen by forming hydrogen bond with the peroxy bond of ILs.

The reusability of catalyst was likewise conducted at mild conditions. As displayed in Fig. 9, the IL could still show the good performance even after five recycles in the epoxidation of cyclooctene, implying that the structure of the IL maintained high stability in the course of reaction, as verified by the similar ⁹³Nb resonance signal as compared that of fresh with spent catalysts (Fig. 6c vs 6d). The ⁹³Nb NMR signal of the reused CE-2 slightly shifted to -980 ppm, which was assigned to less numbers of peroxy groups around niobium sites, as compared to that of fresh CE-2 (-1000 ppm) due to the loss of peroxy groups after the consecutive recycles. Additionally, the FT-IR spectra of the spent CE-2 IL catalyst was almost identical to that of the fresh one (Fig. 2d, right and Fig. S11). Furthermore, the ICP-AES analysis demonstrated that no obvious Nb leaching was monitored (10–20 ppm), which could be responsible for a slight loss of the activity in the successive recycles.

Moreover, the catalytic performance between two CE-derived ILs can

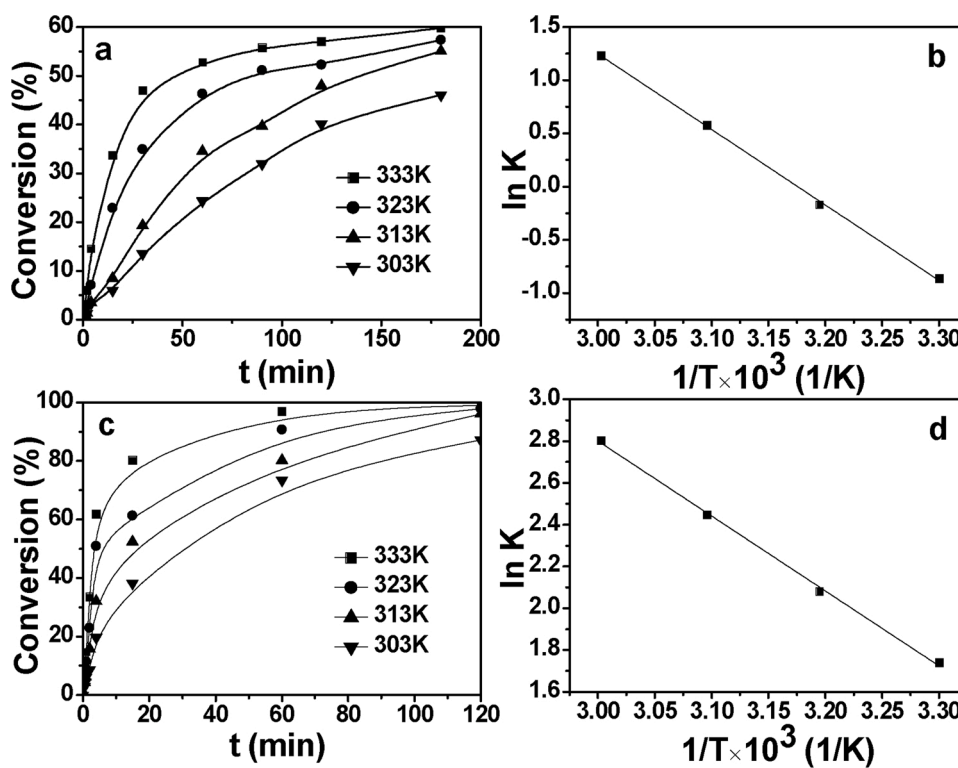

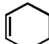
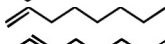
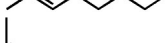
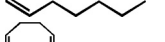
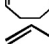
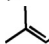

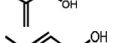
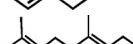
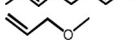
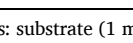
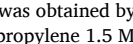


Fig. 8. Conversion/time profiles for the epoxidation reaction by using CE-1 (a) and CE-2 (c) catalysts under various temperatures. Arrhenius plots for epoxidation of cyclooctene of CE-1 (b) and CE-2 (d). The observed rate constants (k) were measured with initial rates accordingly. Reaction conditions: cyclooctene (1 mmol), H₂O₂ (1 mmol), IL catalyst (0.01 mmol), CH₃OH (2 mL), stirring speed (800 rpm).

Table 3
Epoxidation of allylic alcohols and olefins with CE-2.

Entries	Substrates	T/°C	t/h	Con.(%) ^b		Sel.(%)	
						epoxide	others
1		50	3	99	≥99	<1	
2		50	5	65	≥74	<26	
3		50	8	35	≥99	<1	
4		50	8	21	≥99	<1	
5		50	8	81	≥72	<28	
6		50	8	80	≥99	<1	
7 ^c		40	12	32 ^c	≥99	<1	
8 ^d		0	0.5	99	≥99	<1	
9		30	5	90	≥99	<1	
10 ^d		30	5	98	≥99	<1	
11 ^d		30	3	96	≥99	<1	
12		20	2	99	≥99	<1	
13		25	3	60	≥99	<1	

^aReaction conditions: substrate (1 mmol), H₂O₂ (1 mmol), CE-2 (0.01 mmol), 2 mL of CH₃OH.

^b The conversion was obtained by GC with dodecane as an internal standard.

^c Refers to yield, propylene 1.5 MPa.

^d Solvent-free conditions.

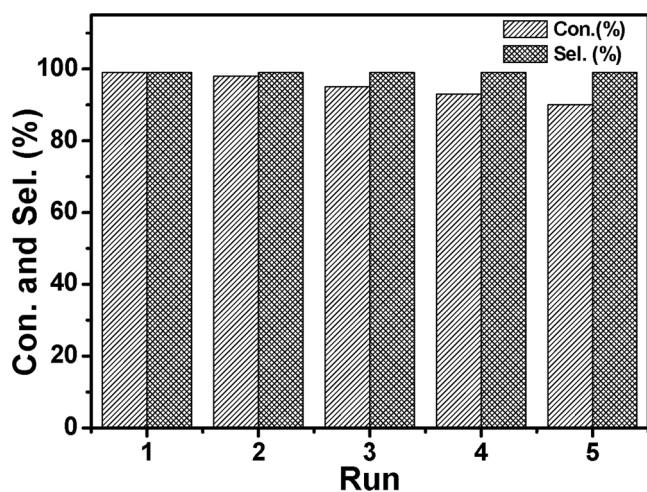
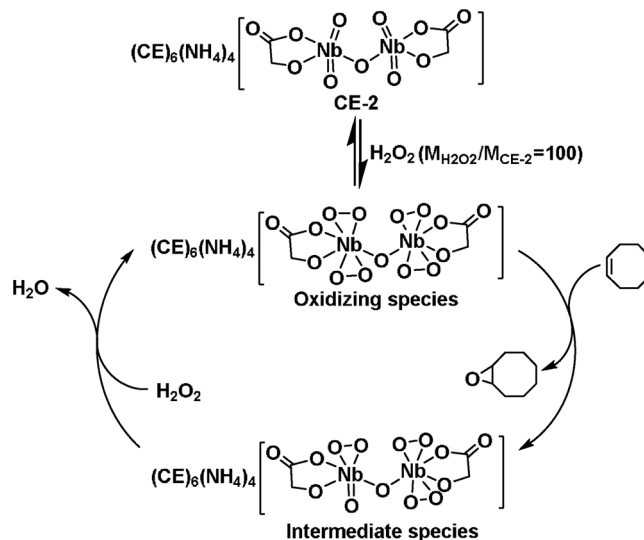


Fig. 9. The recyclability of CE-2 for epoxidation of cyclooctene.

be identified more clearly by the epoxidation of allylic alcohols. As shown in Fig. S12a, CE-2 indeed exhibited much higher activity than CE-1 when 2-buten-1-ol was adopted as model substrate under the identical conditions. As shown from Fig. S12b, there was an obvious difference of CE-1 and CE-2 in the decomposition rates of H₂O₂. Obviously, CE-2 was able to suppress invalid decomposition of H₂O₂ even in the absence of substrates compared with CE-1. This can be ascribed to the coordination of GLY with Nb anion, stabilizing peroxoniobate anion [33,68]. However, CE-1 catalyst can still exhibit moderate to high conversion in epoxidizing allylic alcohols although reaction time was needed to prolong (Table 3 and Table S3). Besides, the epoxidation of long-chain allylic alcohols required methanol as the solvent to achieve high reactivity and selectivity. Especially, the recyclability of the two catalysts was investigated under the optimal conditions for the epoxidation of 3-methyl-2-buten-1-ol. As observed in Fig. S13, the catalytic activity decreased slightly even after five recycles, demonstrating that both of two ILs could maintain high catalytic stability in epoxidizing allylic

alcohols at the present reaction conditions.

Based on the above characterization and activity tests, the reaction pathways were proposed and shown in Scheme 1. The supramolecular IL (CE-2) was derived from CE-1 and the peroxy group of CE-2 was hardly detected by the potential difference titration of Ce³⁺/Ce⁴⁺ (ca. 0.5 peroxy group per Nb atom) (Table 1). The symmetric dimeric structure has further been evidenced by the elemental analysis, MS, FT-IR and ⁹³Nb NMR spectra etc. Next, the IL was oxidized under the action of the excess of H₂O₂, forming oxidizing intermediate species with four peroxy groups (O—O), which was proved by potential difference titration of Ce³⁺/Ce⁴⁺. Afterwards, the C=C double bonds then interacted with the peroxy group to generate epoxides through electrophilic oxygen transfer from the oxidizing species. Meantime, the peroxy group was



Scheme 1. Reaction pathways of cyclooctene epoxidation on the supramolecular IL (CE-2) catalyst. $M_{\text{H}_2\text{O}_2}$ and $M_{\text{CE-2}}$ denoted the molar amounts of H₂O₂ and CE-2 used in the reaction, respectively.

transformed into Nb = O species. From the previous ^{93}Nb NMR spectra, it demonstrated that the interconversion between Nb = O and niobium peroxy groups was completely reversible, which endowed the IL catalyst with good stability and recyclability. Furthermore, the present ILs can obviously improve their miscibility with organic solvent and H_2O_2 , and allowing the facile access of substrates to the catalytically active due to the presence of CE, which enhanced the reaction rate in the process of the epoxidation reaction. Besides, in the crown ether-ammonium ion complexes, it has been reported that the three hydrogens of the NH_4^+ directly interact with the oxygens on the inside of CE by hydrogen-bond interaction while the fourth ammonium hydrogen could be hydrogen bonded to the anion [41]. This specific interaction would decrease the electron density of peroxy (O—O) bond and could be beneficial to the epoxidation reaction by electrophilic oxygen transfer from peroxyoanions [32,33].

4. Conclusions

In this work, we have developed CE (18-crown-6)-derived ILs via the supramolecular complexation between CE and ammonium peroxyoanion in a simple manner. The molar ratio of CE to Nb atom have a vital influence on supramolecular complexation, and it indicated that the specific ILs were formed as the molar ratio of CE to Nb atom was more than 2:1. The parent IL consisting of CE and ammonium peroxyoanion (CE-1) could be further coordinated with GLY by forming five-membered chelate rings to generate a high performance IL (CE-2), which can act as a highly efficient and recoverable catalyst in epoxidizing a series of olefins and allylic alcohols using H_2O_2 at mild conditions. Additionally, it was demonstrated that CE-2 could suppress the degradation of H_2O_2 effectively in comparison with CE-1. Especially, the supramolecular complexation of CE with ammonium ion could play an important role in providing the appropriate hydrophobicity which is beneficial for the easy accessibility of hydrophobic substrates to the active centers. Furthermore, the interconversion between Nb = O and niobium peroxy groups was completely reversible, which was proved by ^{93}Nb NMR and helped us to understand the reaction mechanism thoroughly. The supramolecular ILs exhibited huge advantages in that they were more easily available than that of the previously reported ILs. Undoubtedly, this work represents a vital research subject in the field of green catalysis that can be extended definitely for the efficient catalytic organic transformations via an easily available and sustainable catalytic system.

CCRediT authorship contribution statement

Bingjie Ding: Conceptualization, Methodology, Data curation, Formal analysis, Writing - original draft. **Ran Zhang:** Formal analysis. **Qingqing Zhou:** Formal analysis, Writing - review & editing. **Wenbao Ma:** Investigation, Formal analysis. **Anna Zheng:** Resources. **Difan Li:** Software. **Yefeng Yao:** Methodology, Validation, Visualization. **Zhen-shan Hou:** Funding acquisition, Writing - review & editing, Supervision, Project administration.

Declaration of Competing Interest

The authors reported no declarations of interest.

Acknowledgements

The authors gratefully thank from the National Natural Science Foundation of China (21773061, 21978095). Y. F. acknowledges financial support from Ministry of Science and Technology of the People's Republic of China (Grant No. 2018YFC1602804, 2018YFF01012504) and Microscale Magnetic Resonance Platform of ECNU.

Appendix A. Supplementary data

Supplementary material related to this article can be found, in the online version, at doi:<https://doi.org/10.1016/j.mcat.2020.111342>.

References

- [1] D.T. Bregante, N.E. Thornburg, J.M. Notestein, D.W. Flaherty, Consequences of confinement for alkene epoxidation with hydrogen peroxide on highly dispersed group 4 and 5 metal oxide catalysts, *ACS Catal.* 8 (2018) 2995–3010, <https://doi.org/10.1021/acscatal.7b03986>.
- [2] W.B. Cunningham, J.D. Tibbetts, M. Hutchby, K.A. Maltby, M.G. Davidson, U. Hintermair, P. Plucinski, S.D. Bull, Sustainable catalytic protocols for the solvent free epoxidation and anti-dihydroxylation of the alkene bonds of biorenewable terpene feedstocks using H_2O_2 as oxidant, *Green Chem.* 22 (2020) 513–524, <https://doi.org/10.1039/C9GC03208H>.
- [3] Y. Jia, Z.A. Allothman, R. Liang, S. Cha, X. Li, W. Ouyang, A. Zheng, S.M. Osman, R. Luque, Y. Sun, Immobilization of (tartrate-salen)Mn(III) polymer complexes into SBA-15 for catalytic asymmetric epoxidation of alkenes, *Mol. Catal.* 495 (2020) 111146–111155, <https://doi.org/10.1016/j.mcat.2020.111146>.
- [4] K. Kamata, K. Sugahara, R. Ishimoto, S. Nojima, M. Okazaki, T. Matsumoto, N. Mizuno, Highly selective epoxidation of cycloaliphatic alkenes with aqueous hydrogen peroxide catalyzed by $[\text{PO}_4\{\text{WO}(\text{O}_2)_2\}_4]^{3-}$ /imidazole, *ChemCatChem* 6 (2014) 2327–2332, <https://doi.org/10.1002/cctc.201402268>.
- [5] J. Chen, Z. Jiang, S. Fukuzumi, W. Nam, B. Wang, Artificial nonheme iron and manganese oxygenases for enantioselective olefin epoxidation and alkane hydroxylation reactions, *Coord. Chem. Rev.* 421 (2020) 213443–213470, <https://doi.org/10.1016/j.ccr.2020.213443>.
- [6] B.S. Lane, K. Burgess, Metal-catalyzed epoxidations of alkenes with hydrogen peroxide, *Chem. Rev.* 103 (2003) 2457–2473, <https://doi.org/10.1021/cr020471z>.
- [7] W. Cheng, X. Wang, G. Li, X. Guo, S. Zhang, Highly efficient epoxidation of propylene to propylene oxide over TS-1 using urea + hydrogen peroxide as oxidizing agent, *J. Catal.* 255 (2008) 343–346, <https://doi.org/10.1016/j.jcat.2008.02.018>.
- [8] L. Davies, P. McMorn, D. Bethell, P.C. Bulman Page, F. King, F.E. Hancock, G. J. Hutchings, Effect of preparation method on leaching of Ti from the redox molecular sieve TS-1, *Phys. Chem. Chem. Phys.* 3 (2001) 632–639, <https://doi.org/10.1039/B007651L>.
- [9] C.R. Goldsmith, Aluminum and gallium complexes as homogeneous catalysts for reduction/oxidation reactions, *Coord. Chem. Rev.* 377 (2018) 209–224, <https://doi.org/10.1016/j.ccr.2018.08.025>.
- [10] M. Amini, M.M. Haghdoost, M. Bagherzadeh, Monomeric and dimeric oxido-peroxido tungsten(VI) complexes in catalytic and stoichiometric epoxidation, *Coord. Chem. Rev.* 268 (2014) 83–100, <https://doi.org/10.1016/j.ccr.2014.01.035>.
- [11] A. Dupé, M.K. Hossain, J.A. Schachner, F. Belaj, A. Lehtonen, E. Nordlander, N. C. Mösch-Zanetti, Dioxomolybdenum(VI) and -tungsten(VI) complexes with multidentate aminobisphenol ligands as catalysts for olefin epoxidation, *Eur. J. Inorg. Chem.* 2015 (2015) 3572–3579, <https://doi.org/10.1002/ejic.201500055>.
- [12] A. Schmidt, N. Grover, T.K. Zimmermann, L. Graser, M. Cokoja, A. Pöthig, F. E. Kühn, Synthesis and characterization of novel cyclopentadienyl molybdenum imidazo[1,5-a]pyridine-3-ylidene complexes and their application in olefin epoxidation catalysis, *J. Catal.* 319 (2014) 119–126, <https://doi.org/10.1016/j.jcat.2014.08.013>.
- [13] N. Zwitter, J.A. Schachner, F. Belaj, N.C. Mösch-Zanetti, Hydrogen bond donor functionalized dioxido-molybdenum(VI) complexes as robust and highly efficient precatalysts for alkene epoxidation, *Mol. Catal.* 443 (2017) 209–219, <https://doi.org/10.1016/j.mcat.2017.09.036>.
- [14] W. Yan, G. Zhang, H. Yan, Y. Liu, X. Chen, X. Feng, X. Jin, C. Yang, Liquid-phase epoxidation of light olefins over W and Nb nanocatalysts, *ACS Sustain. Chem. Eng.* 6 (2018) 4423–4452, <https://doi.org/10.1021/acssuschemeng.7b03101>.
- [15] S. Ishikawa, Y. Maegawa, M. Waki, S. Inagaki, Immobilization of a molybdenum complex on bipyrindine-based periodic mesoporous organosilica and its catalytic activity for epoxidation of olefins, *ACS Catal.* 8 (2018) 4160–4169, <https://doi.org/10.1021/acscatal.8b00809>.
- [16] C. Copéret, A. Comas-Vives, M.P. Conley, D.P. Estes, A. Fedorov, V. Mougél, H. Nagae, F. Núñez-Zarur, P.A. Zhizhko, Surface organometallic and coordination chemistry toward single-site heterogeneous catalysts: strategies, methods, structures, and activities, *Chem. Rev.* 116 (2016) 323–421, <https://doi.org/10.1021/acs.chemrev.5b00373>.
- [17] P. Carniti, A. Gervasini, C. Tiozzo, M. Guidotti, Niobium-containing hydroxyapatites as amphoteric catalysts: synthesis, properties, and activity, *ACS Catal.* 4 (2014) 469–479, <https://doi.org/10.1021/cs4010453>.
- [18] N.E. Thornburg, S.L. Nauert, A.B. Thompson, J.M. Notestein, Synthesis–structure–function relationships of silica-supported Niobium(V) catalysts for alkene epoxidation with H_2O_2 , *ACS Catal.* 6 (2016) 6124–6134, <https://doi.org/10.1021/acscatal.6b01796>.
- [19] N.E. Thornburg, A.B. Thompson, J.M. Notestein, Periodic trends in highly dispersed groups IV and V supported metal oxide catalysts for alkene epoxidation with H_2O_2 , *ACS Catal.* 5 (2015) 5077–5088, <https://doi.org/10.1021/acscatal.5b01105>.
- [20] H. Egami, T. Oguma, T. Katsuki, Oxidation catalysis of Nb(salan) complexes: asymmetric epoxidation of allylic alcohols using aqueous hydrogen peroxide as an

- oxidant, *J. Am. Chem. Soc.* 132 (2010) 5886–5895, <https://doi.org/10.1021/ja100795k>.
- [21] D.C. Batalha, N.H. Marins, R.M. Silva, N.L.V. Carreño, H.V. Fajardo, M.J. Silva, Oxidation of terpenic alcohols with hydrogen peroxide promoted by Nb₂O₅ obtained by microwave-assisted hydrothermal method, *Mol. Catal.* 489 (2020) 110941–110952, <https://doi.org/10.1016/j.mcat.2020.110941>.
- [22] Y. Qiao, W. Ma, N. Theyssen, C. Chen, Z. Hou, Temperature-responsive ionic liquids: fundamental behaviors and catalytic applications, *Chem. Rev.* 117 (2017) 6881–6928, <https://doi.org/10.1021/acs.chemrev.6b00652>.
- [23] G. Chen, J. Zhang, X. Chen, X. Tan, J. Shi, D. Tan, B. Zhang, Q. Wan, F. Zhang, L. Liu, B. Han, G. Yang, Metal ionic liquids for the rapid chemical fixation of CO₂ under ambient conditions, *ChemCatChem* 12 (2020) 1963–1967, <https://doi.org/10.1002/cctc.201902347>.
- [24] J.P. Hallett, T. Welton, Room-temperature ionic liquids: solvents for synthesis and catalysis, *Chem. Rev.* 111 (2011) 3508–3576, <https://doi.org/10.1021/cr1003248>.
- [25] B.C. Leal, C.S. Consorti, G. Machado, J. Dupont, Palladium metal nanoparticles stabilized by ionophilic ligands in ionic liquids: synthesis and application in hydrogenation reactions, *Catal. Sci. Technol.* 5 (2015) 903–909, <https://doi.org/10.1039/C4CY01116C>.
- [26] J.L. Shamshina, G. Gurau, L.E. Block, L.K. Hansen, C. Dingee, A. Walters, R. D. Rogers, Chitin–calcium alginate composite fibers for wound care dressings spun from ionic liquid solution, *J. Mater. Chem. B* 2 (2014) 3924–3936, <https://doi.org/10.1039/C4TB00329B>.
- [27] J. Gräsvik, J.P. Hallett, T.Q. To, T. Welton, A quick, simple, robust method to measure the acidity of ionic liquids, *Chem. Commun.* 50 (2014) 7258–7261, <https://doi.org/10.1039/C4CC02816C>.
- [28] Y. Li, X. Zhang, Z. Li, J. Song, X. Wang, Full utilization of lignocellulose with ionic liquid polyoxometalates in a one-pot three-step conversion, *ChemSusChem* 12 (2019) 1–11, <https://doi.org/10.1002/cssc.201902503>.
- [29] S. Herrmann, L.D. Matteis, J.M. de la Fuente, S.G. Mitchell, C. Streb, Removal of multiple contaminants from water by polyoxometalate supported ionic liquid phases (POM-SILPs), *Angew. Chem. Int. Ed.* 56 (2017) 1667–1670, <https://doi.org/10.1002/anie.201611072>.
- [30] B.B.A. Bediako, Q. Qian, J. Zhang, Y. Wang, X. Shen, J. Shi, M. Cui, G. Yang, Z. Wang, S. Tong, B. Han, Ru-catalyzed methanol homologation with CO₂ and H₂ in an ionic liquid, *Green Chem.* 21 (2019) 4152–4158, <https://doi.org/10.1039/C9GC01185D>.
- [31] V.S. Souza, J.D. Scholten, D.E. Weibel, D. Eberhardt, D.L. Baptista, S.R. Teixeira, J. Dupont, Hybrid tantalum oxide nanoparticles from the hydrolysis of imidazolium tantalate ionic liquids: efficient catalysts for hydrogen generation from ethanol/water solutions, *J. Mater. Chem. A* 4 (2016) 7469–7475, <https://doi.org/10.1039/C6TA02114J>.
- [32] C. Chen, H. Yuan, H. Wang, Y. Yao, W. Ma, J. Chen, Z. Hou, Highly efficient epoxidation of allylic alcohols with hydrogen peroxide catalyzed by peroxoniobate-based ionic liquids, *ACS Catal.* 6 (2016) 3354–3364, <https://doi.org/10.1021/acscatal.6b00786>.
- [33] W. Ma, H. Yuan, H. Wang, Q. Zhou, K. Kong, D. Li, Y. Yao, Z. Hou, Identifying catalytically active mononuclear peroxoniobate anion of ionic liquids in the epoxidation of Olefins, *ACS Catal.* 8 (2018) 4645–4659, <https://doi.org/10.1021/acscatal.7b04443>.
- [34] G. Benay, G. Wipff, Ammonium recognition by 18-crown-6 in different solutions and at an aqueous interface: a simulation study, *J. Phys. Chem. B* 118 (2014) 13913–13929, <https://doi.org/10.1021/jp508379w>.
- [35] D. Yu, T. Mu, Strategy to form eutectic molecular liquids based on noncovalent interactions, *J. Phys. Chem. B* 123 (2019) 4958–4966, <https://doi.org/10.1021/acs.jpcc.9b02891>.
- [36] M. Gao, Y. Wang, Q. Yi, Y. Su, P. Sun, X. Wang, J. Zhao, G. Zou, A novel solid-state electrolyte based on a crown ether lithium salt complex, *J. Mater. Chem. A* 3 (2015) 20541–20546, <https://doi.org/10.1039/C5TA04933D>.
- [37] Y. Song, H. Jing, B. Li, D. Bai, Crown ether complex cation ionic liquids: preparation and applications in organic reactions, *Chem. Eur. J.* 17 (2011) 8731–8738, <https://doi.org/10.1002/chem.201100112>.
- [38] T. Xiao, L. Xu, L. Zhou, X.Q. Sun, C. Lin, L. Wang, Dynamic hydrogels mediated by macrocyclic host–guest interactions, *J. Mater. Chem. B* 7 (2019) 1526–1540, <https://doi.org/10.1039/C8TB02339E>.
- [39] D.A. Fowler, C.R. Pfeiffer, S.J. Teat, C.M. Beavers, G.A. Baker, J.L. Atwood, Illuminating host–guest cocrystallization between pyrogallol[4]arenes and the ionic liquid 1-ethyl-3-methylimidazolium ethylsulfate, *CrystEngComm* 16 (2014) 6010–6022, <https://doi.org/10.1039/C4CE00359D>.
- [40] W. Ma, C. Chen, K. Kong, Q. Dong, K. Li, M. Yuan, D. Li, Z. Hou, Peroxotantalate-based ionic liquid catalyzed epoxidation of allylic alcohols with hydrogen peroxide, *Chem. Eur. J.* 23 (2017) 7287–7296, <https://doi.org/10.1002/chem.201605661>.
- [41] A. Chen, C. Chen, Y. Xiu, X. Liu, J. Chen, L. Guo, R. Zhang, Z. Hou, Niobate salts of organic base catalyzed chemical fixation of carbon dioxide with epoxides to form cyclic carbonates, *Green Chem.* 17 (2015) 1842–1852, <https://doi.org/10.1039/C4GC02244K>.
- [42] D. Bayot, B. Tinant, M. Devillers, Water-soluble niobium peroxo complexes as precursors for the preparation of Nb-based oxide catalysts, *Catal. Today* 78 (2003) 439–447, [https://doi.org/10.1016/S0920-5861\(02\)00325-5](https://doi.org/10.1016/S0920-5861(02)00325-5).
- [43] K. Kamata, K. Yamaguchi, N. Mizuno, Highly selective, recyclable epoxidation of allylic alcohols with hydrogen peroxide in water catalyzed by dinuclear peroxotungstate, *Chem. Eur. J.* 10 (2004) 4728–4734, <https://doi.org/10.1002/chem.200400352>.
- [44] C. Endicott, H.L. Strauss, Infrared hole burning of crown ether 18-c-6 ammonium ion complexes, *J. Phys. Chem. A* 111 (2007) 1236–1244, <https://doi.org/10.1021/jp0658795>.
- [45] D. Yu, H. Mou, H. Fu, X. Lan, Y. Wang, T. Mu, “Inverted” deep eutectic solvents based on host–guest interactions, *Chem. Asian J.* 14 (2019) 4183–4188, <https://doi.org/10.1002/asia.201901365>.
- [46] M.G. Mohamed, S.-W. Kuo, Crown ether-functionalized polybenzoxazine for metal ion adsorption, *Macromolecules* 53 (2020) 2420–2429, <https://doi.org/10.1021/acs.macromol.9b02519>.
- [47] Z.-Z. Yang, D. Jiang, X. Zhu, C. Tian, S. Brown, C.-L. Do-Thanh, L.-N. He, S. Dai, Coordination effect-regulated CO₂ capture with an alkali metal onium salts/crown ether system, *Green Chem.* 16 (2014) 253–258, <https://doi.org/10.1039/C3GC41513A>.
- [48] D. Bayot, M. Devillers, D. Peeters, Vibrational spectra of eight-coordinate niobium and tantalum complexes with peroxo ligands: a theoretical simulation, *Eur. J. Inorg. Chem.* 2005 (2005) 4118–4123, <https://doi.org/10.1002/ejic.200500428>.
- [49] Z. Yan, X. Lin, H. Guo, F. Yang, A novel fluorescence sensor for K⁺ based on bis-Bodipy: the ACQ effect controlled by cation complexation of pseudo crown ether ring, *Tetrahedron Lett.* 58 (2017) 3064–3068, <https://doi.org/10.1016/j.tetlet.2017.06.065>.
- [50] L. Patron, O. Carp, I. Mindru, G. Marinescu, E. Segal, Iron, nickel and zinc malates coordination compounds synthesis, characterization and thermal behaviour, *J. Therm. Anal. Cal.* 72 (2003) 281–288, <https://doi.org/10.1023/A:1023948526145>.
- [51] A. Felicke, G. Meijer, G. Helden, Infrared spectroscopy of niobium oxide cluster cations in a molecular beam: identifying the cluster structures, *J. Am. Chem. Soc.* 125 (2003) 3659–3667, <https://doi.org/10.1021/ja0288946>.
- [52] G. Xu, F. Hao, M. Weng, J. Hong, F. Pan, D. Fang, Strong influence of strain gradient on lithium diffusion: flexo-diffusion effect, *Nanoscale* 12 (2020) 15175–15184, <https://doi.org/10.1039/D0NR03746J>.
- [53] L. Garrido, I. Aranz, A. Gallardo, C. García, N. García, E. Benito, J. Guzmán, Ionic conductivity, diffusion coefficients, and degree of dissociation in lithium electrolytes, ionic liquids, and hydrogel polyelectrolytes, *J. Phys. Chem. B* 122 (2018) 8301–8308, <https://doi.org/10.1021/acs.jpcc.8b06424>.
- [54] S. Saha, M.N. Roy, Exploration of complexes of 18-crown-6 with three similarly substituted imidazolium, pyridinium and pyrrolidinium ionic liquids, *Chem. Phys. Lett.* 684 (2017) 44–52, <https://doi.org/10.1016/j.cplett.2017.06.037>.
- [55] M. Zanatta, V.U. Antunes, C.F. Tormena, J. Dupont, F.P. dos Santos, Dealing with supramolecular structure for ionic liquids: a DOSY NMR approach, *Phys. Chem. Chem. Phys.* 21 (2019) 2567–2571, <https://doi.org/10.1039/C8CP07071G>.
- [56] H. Barańska, J. Kuduk-Jaworska, R. Szostak, A. Romaniewska, Vibrational spectra of racemic and enantiomeric malic acids, *J. Raman Spectrosc.* 34 (2003) 68–76, <https://doi.org/10.1002/jrs.953>.
- [57] D. Bayot, B. Tinant, M. Devillers, Homo- and heterobimetallic niobium^v and tantalum^v peroxo-tartrate complexes and their use as molecular precursors for Nb-Ta mixed oxides, *Inorg. Chem.* 44 (2005) 1554–1562, <https://doi.org/10.1021/ic0484250>.
- [58] C.P. Reghunadhan Nair, P.K. Manshad, A.M. Ashir, S. Athul, Synthesis of 3-carbononyl acrylic acid-functionalized polystyrene and an insight in to its role in cross linking and grafting of polystyrene on to natural rubber, *Eur. Polym. J.* 131 (2020) 109687–109696, <https://doi.org/10.1016/j.eurpolymj.2020.109688>.
- [59] C. Chen, X. Zhao, J. Chen, L. Hua, R. Zhang, L. Guo, B. Song, H. Gan, Z. Hou, Niobium peroxide-catalyzed selective epoxidation of allylic alcohols, *ChemCatChem* 6 (2014) 3231–3238, <https://doi.org/10.1002/cctc.201402545>.
- [60] F. Liu, L. Wang, Q. Sun, L. Zhu, X. Meng, F.-S. Xiao, Transesterification catalyzed by ionic liquids on superhydrophobic mesoporous polymers: heterogeneous catalysts that are faster than homogeneous catalysts, *J. Am. Chem. Soc.* 134 (2012) 16948–16950, <https://doi.org/10.1021/ja307455w>.
- [61] A. Solé-Daura, T. Zhang, H. Fouilloux, C. Robert, C.M. Thomas, L.-M. Chamoreau, J.J. Carbó, A. Proust, G. Guillemot, J.M. Poblet, Catalyst design for alkene epoxidation by molecular analogues of heterogeneous titanium-silicalite catalysts, *ACS Catal.* 10 (2020) 4737–4750, <https://doi.org/10.1021/acscatal.9b05147>.
- [62] Y. Qiao, Z. Hou, H. Li, Y. Hu, B. Feng, X. Wang, L. Hua, Q. Huang, Polyoxometalate-based protic alkyimidazolium salts as reaction-induced phase-separation catalysts for olefin epoxidation, *Green Chem.* 11 (2009) 1955–1960, <https://doi.org/10.1039/B916766H>.
- [63] Y. Cao, H. Yu, H. Wang, F. Peng, Solvent effect on the allylic oxidation of cyclohexene catalyzed by nitrogen doped carbon nanotubes, *Catal. Commun.* 88 (2017) 99–103, <https://doi.org/10.1016/j.catcom.2016.10.002>.
- [64] M. Ziolk, P. Decyk, I. Sobczak, M. Trejda, J. Florek, H.G.W. Klimas, A. Wojtaszek, Catalytic performance of niobium species in crystalline and amorphous solids—gas and liquid phase oxidation, *Appl. Catal. A Gen.* 391 (2011) 194–204, <https://doi.org/10.1016/j.apcata.2010.07.022>.
- [65] M. Ziolk, I. Sobczak, P. Decyk, K. Sobanska, P. Pietrzyk, Z. Sojka, Search for reactive intermediates in catalytic oxidation with hydrogenperoxide over amorphous niobium(V) and tantalum(V) oxides, *Appl. Catal. B* 164 (2015) 288–296, <https://doi.org/10.1016/j.apcatb.2014.09.024>.
- [66] H. Alshammari, P.J. Miedziak, T.E. Davies, D.J. Willock, D.W. Knight, G. J. Hutchings, Initiator-free hydrocarbon oxidation using supported gold

- nanoparticles, *Catal. Sci. Technol.* 4 (2014) 908–911, <https://doi.org/10.1039/C4CY00088A>.
- [67] M. Papastergiou, P. Stathi, E.R. Milaeva, Y. Deligiannakis, M. Loulodi, Comparative study of the catalytic thermodynamic barriers for two homologous Mn- and Fe-non-heme oxidation catalysts, *J. Catal.* 341 (2016) 104–115, <https://doi.org/10.1016/j.jcat.2016.06.017>.
- [68] C. Djordjević, N. Vuletić, Coordination complexes of niobium and tantalum. V. eight-coordinated di- and triperoxoniobates(V) and -tantalates(V) with some nitrogen and oxygen bidentate ligands, *Inorg. Chem.* 7 (1968) 1864–1868, <https://doi.org/10.1021/ic50067a033>.